Small-Angle X-ray Scattering Studies of Fe-Montmorillonite Deposits during Ultrafiltration in a Magnetic Field

ARTICLE *in* LANGMUIR · SEPTEMBER 2003

Impact Factor: 4.46 · DOI: 10.1021/la030020p

4 AUTHORS, INCLUDING:

Frédéric Pignon
University Joseph Fourier - Grenoble 1
84 PUBLICATIONS **1,173** CITATIONS
SEE PROFILE

Albert Magnin
French National Centre for Scientific Research
169 PUBLICATIONS **2,329** CITATIONS
SEE PROFILE

Small-Angle X-ray Scattering Studies of Fe-Montmorillonite Deposits during Ultrafiltration in a Magnetic Field

Frédéric Pignon,*,† Ayse Alemdar,† Albert Magnin,† and Theyencheri Narayanan‡

Laboratoire de Rhéologie, Université Joseph Fourier Grenoble I, Institut National Polytechnique de Grenoble, CNRS UMR 5520, BP 53, 38041 Grenoble Cedex 9, France, and European Synchrotron Radiation Facility, BP 220, F-38043 Grenoble Cedex, France

Received January 21, 2003. In Final Form: July 21, 2003

This paper presents a small-angle X-ray scattering (SAXS) characterization of the structural organization of deposits of Fe-montmorillonite dispersions formed during frontal ultrafiltration in a magnetic field. The mineral colloidal dispersions are made up of platelike montmorillonite clay particles with average thickness and diameter of about 2 and 500 nm, respectively. A newly developed X-ray-compatible frontal ultrafiltration cell allowed simultaneously applying a transmembrane pressure (5×10^4 Pa) and a magnetic field. The Fe-montmorillonite dispersions obtained by cation exchange reaction displayed regular ordering of the particles with an anisotropic arrangement when subjected to a uniform magnetic field of strengths ranging up to 1.4 T. The degree of anisotropy and the particle concentration profiles as a function of the distance from the filter membrane were deduced from the measured SAXS intensity. For the same volume of filtered permeate (0.26 mL), the deposit formed in a magnetic field of 1 T exhibits an anisotropic arrangement of the platelike particles with their faces aligned parallel to the membrane. In the absence of a magnetic field, the deposits are composed of randomly oriented particles. The application of an external magnetic field produced uniaxially oriented deposits with a higher concentration of particles, and resulted in a higher permeation flow than in the absence of the field.

Introduction

Understanding the mechanisms involved in the structural organization of colloidal particles subjected simultaneously to filtration and an external magnetic field is relevant in many processing applications involved in microelectronics, ceramics, bio- and agro-industries, sludge treatment, and so forth. The packing and the orientation of colloidal particles during the processing (involving deposition, ultrafiltration, extrusion, etc.) have a direct influence on the final macroscopic optical, mechanical, or electrical properties of the fabricated material as well as the performance of the processing. For example, in the case of membrane separation, an important factor which controls the efficiency of the filtration is the structural characteristics of the deposits near the separating membrane, in relation to the magnitude of the permeate flow rate. During the past few years, many experimental works[1,2] and theoretical models[3−5] have been reported. Nevertheless, few attempts have been made to characterize the structural organization of the deposits, which controls the performance of the filtration process.[6−9]

The goal of this paper is first to characterize the structural organization of deposits of Fe-montmorillonite dispersions as a function of time and second to control the structural arrangement of the particles by the application of an external magnetic field during the filtration process. The consequences are several: controlling the particle organization can be used to fabricate new types of dense colloidal materials with anisotropic structural, mechanical, or electrical properties, and understanding the structural organization of the deposit helps in enhancing filtration performance. To probe the mechanism of arrangement of colloidal particles under the influence of a magnetic field, in situ small-angle X-ray scattering (SAXS) measurements were performed during the frontal ultrafiltration process. Using SAXS and a newly developed cell filtration it became possible to monitor and fine-tune the structural organization of the deposits during the filtration process in a magnetic field. The material used here consisted of an aqueous Fe-montmorillonite dispersion, composed of platelike particles of average thickness and diameter about 2 and 500 nm, respectively. Synchrotron SAXS measurements using a highly collimated beam (0.1 mm × 0.3 mm) provided time-resolved structural information as a function of distance from the filtration membrane with a resolution of 0.1 mm.

This paper reports measurements performed both under static conditions (in a capillary) and with a differential air pressure of 5×10^4 Pa in the filtration cell. With controlled physicochemical parameters (pH, ionic strength) and a fixed filtration pressure, external magnetic fields of different strengths (**B**) were applied. In static conditions, without the magnetic field ($\mathbf{B} = 0$), the system consists of randomly oriented particles. In a magnetic field, **B** ranging from 0.01 to 1.43 T, particles orient uniaxially with increasing anisotropy with the field. Using a filtration cell without a magnetic field, measurements showed that the deposits are composed of randomly oriented particles

* Corresponding author. E-mail: Pignon@ujf-grenoble.fr.
† Université Joseph Fourier Grenoble I.
‡ European Synchrotron Radiation Facility.

(1) Bacchin, P.; Aimar, P.; Sanchez, V. *AIChE J.* **1995**, *41*, 368−376.
(2) Waite, T. D.; Schäfer, A. I.; Fane, A. G.; Heuer, A. *J. Colloid Interface Sci.* **1999**, *212*, 264−274.
(3) Bowen, W. R.; Jenner, F. *Chem. Eng. Sci.* **1995**, *50*, 1707−1735.
(4) Bowen, W. R.; Mongruel, A.; Williams, P. M. *Chem. Eng. Sci.* **1996**, *51*, 4321−4333.
(5) Jönsson, A. S.; Jönsson, B. *J. Colloid Interface Sci.* **1996**, *1801*, 504−518.
(6) Pignon, F.; Magnin, A.; Piau, J. M.; Cabane, B.; Aimar, P.; Meireles M.; Lindner, P. *J. Membr. Sci.* **2000**, *174*, 189−204.
(7) Su, T. J.; Lu, J. R.; Cui, Z. F.; Thomas, R. K.; Heenan, R. K. *Langmuir* **1998**, *14*, 5517−5520.
(8) Stefanopolous, J. L.; Romanos, G. E.; Mitropolous, A. Ch.; Kanellopoulos, N. K.; Heenan, R. K. *J. Membr. Sci.* **1999**, *153*, 1−7.
(9) Antelmi, D.; Cabane, B.; Meireles, M.; Aimar, P. *Langmuir* **2001**, *17*, 7137−7144.

10.1021/la030020p CCC: $25.00
Published on Web 09/06/2003

with increasing particle concentrations near the membrane. In a magnetic field of 1 T, the deposits consisted of particles regularly oriented parallel to the membrane. Simultaneously, the filtration flow rate was enhanced with the applied magnetic field. Concentration profiles and the anisotropy parameter were deduced from scattering measurements as a function of distance from the membrane during the filtration process.

The results obtained in this paper provide a better insight into colloidal material processing. First of all, this method enables dense colloidal materials with anisotropic structural, mechanical, or electrical properties to be fabricated. Second, the organization of the particles during the filtration process can be controlled, thereby enhancing the efficiency of the separation methods.[1,6−10] Third, the quantitative data obtained from these measurements provide new opportunities to correlate experimental data with theoretical and numerical predictions and permeation flow rate measurements.[11,12]

Materials and Methods

Materials. Clay minerals, such as purified natural montmorillonite, are composed of stacks of alumina and silica sheets joined together. Two structural units are involved in the atomic lattices of montmorillonite. The unit cell of montmorillonite consists of a combination of one octahedral and two tetrahedral sheets.[13] Clay mineral crystals carry a charge arising from the isomorphous substitution of certain elements in their structure for other ions of a different valency. In the tetrahedral sheet, Si^{4+} can be replaced by trivalent cations (Al^{3+} or Fe^{3+}), or divalent cations (Mg^{2+} or Fe^{2+}) can be replaced by Al^{3+} in the octahedral sheet. In this case, a charge deficiency results that leads to negative charge at the surface of the clay. The negative charge is compensated by the adsorption of exchangeable cations on the surface. The total amount of cations adsorbed by the clay, expressed in milliequivalents per hundred grams of dry clay, is called the cation exchange capacity (CEC). The CEC is high for sodium montmorillonite compared to the other clay minerals. With this in perspective, several attempts to produce transition metal particles between the layers of montmorillonite have been described in the literature.[14,15]

The purified clay samples were obtained from the bentonite deposits in Enez, Turkey (Bensan Co.). The clay mineral types were determined by X-ray diffraction (Philips PW 1040 model X-ray diffractometer). The dominant clay mineral was found to be the dioctahedral montmorillonite with minor amounts of illite and kaolinite. Small amounts of quartz were always present in the clay fractions. Sodium montmorillonite was prepared from the corresponding bentonites with the following treatments: First, iron oxides were removed by sodium citrate and sodium dithionate buffering reactions. To remove the carbonates, a bentonite dispersion was mixed with NaCl/HCl solution and repeatedly washed with fresh solution. Organic materials were oxidized with hydrogen peroxide solution at 80 °C. The particles greater than 2 μm were fractionated out by sedimentation under gravity. The resulting dispersion was then saturated with sodium, dialyzed, and freeze-dried.[16,17] The layer charge determined by the alkylammonium titration was 0.283 (equiv/mol). The cation exchange capacity of montmorillonite is 0.7 mequiv/g.[18]

The chemical composition of the purified montmorillonite clay particles is as follows: SiO_2, 62.6%; Al_2O_3, 19.3%; Fe_2O_3, 6.1%; Na_2O, 2.4%; CaO, 0.2%; K_2O, 0.7%; MgO, 2.5%; MnO, 0.01%; TiO_2, 0.8%; P_2O_5, 0.04%. The particle size distribution in the clay samples was determined by a Malvern Mastersizer. The particles were suspended in distilled water and homogeneously dispersed by ultrasonic agitation for 10 min. One principal peak was observed in the size distributions for the purified montmorillonite and the Fe-montmorillonite dispersion in the 100−1000 nm range with a maximum at 500 nm. The zeta potentials of purified montmorillonite and Fe-montmorillonite as measured by electrophoretic mobility using a Malvern Zetasizer 5000 were −38.9 and −38.8 mV, respectively.

Cation Exchange Procedure. To orient the montmorillonite particles in a magnetic field, purified montmorillonite particles were saturated with Fe^{2+} ions by cation exchange to give paramagnetic properties to the clay particles. Uyeda et al.[19] studied the diamagnetic orientation of clay mineral grains in a magnetic field. They observed that the disk-shaped grains are oriented parallel to the magnetic field. The magnetic properties of these grains can be manipulated for tailored applications by altering the volume fraction of the magnetic component. Production of transition metal particles in clay minerals has been of considerable interest in the past.[20,21] Recently, Esmer and Yeniyol[22] showed that sepiolite saturated with Fe^{2+} cations by cation exchange can be oriented in a magnetic field.

To implant paramagnetic properties in the montmorillonite particles, the following cation exchange procedure was used. First, montmorillonite samples were mechanically dispersed (Ultra Turrax T25 basik) and leached by washing several times with doubly deionized water and centrifuging the suspension (3500 rpm for 30 min). The samples were then dispersed using Labsonic ultrasonic equipment with a high-intensity sonic probe (300 W) with a pulse duration of 0.3 s for 5 min. In the next step, 5 g of montmorillonite was dispersed in an excess molar amount (3 times the cation exchange capacity) of $Fe_2(SO_4)_3 \cdot 5H_2O$ (Aldrich) solution. The mixture was stirred (at 150 rpm for 20 h) by a mechanical stirrer with a deflocculating vane at room temperature. Then the mixture was centrifuged (3500 rpm, 15 min) (Heraeus Instruments, Biofuge stratos) and the supernatant was discarded. This procedure was repeated three times to complete the ion exchange reaction. After the cation exchange procedure, the sediment was washed several times with doubly deionized water to remove the excess salts. This washing procedure was repeated until the clay dispersion became stable with respect to aggregation and precipitation. The sediment of Fe-montmorillonite was then baked in an oven at 50 °C.

Purified montmorillonite and Fe-montmorillonite, which were obtained after the cation exchange procedure, were characterized by scanning electron microscopy (SEM). Electron diffraction experiments showed that the Fe ratio was 6% in the purified montmorillonite, which increased to 15% as a result of additional Fe introduced by the cation exchange procedure.

For the filtration and SAXS experiments, aqueous suspensions of purified montmorillonite and Fe-montmorillonite of concentration (C) 10^{-3} g mL^{-1} were prepared by dispersing the montmorillonite particles in doubly deionized water by ultrasound treatment for 5 min followed by overnight (12 h) shaking (Heidolph Instruments Promax 2020). Before the filtration experiment, the suspension was treated with ultrasound for an additional hour and then left undisturbed for 24 h. The pH of the dispersions was 6.5 at 24 °C.

The Filtration Cell in the Magnetic Field. The filtration cell shown in Figure 1 was specially designed to probe the formation of deposits by SAXS. The rectangular cell is made of polycarbonate with inner dimensions 4 mm × 1 mm × 38 mm. To reduce absorption and parasitic scattering, the cell wall thickness was reduced to 0.5 mm along the entire window over which the X-ray beam probed the sample above the filter (up to

(10) Malaescu, I.; Gabor, L.; Claici, F.; Stefu, N. *J. Magn. Magn. Mater.* **2000**, *222*, 8−12.
(11) Kozinski, A. A.; Lightfoot, E. N. *AIChE J.* **1972**, *18*, 1030−1040.
(12) Song, L.; Elimelech, M. *J. Chem. Soc., Faraday Trans.* **1995**, *91*, 3389−3398.
(13) Searle, B. A.; Grimshaw, R. W. *The Chemistry and Physics of Clays and other Ceramic Materials*; Ernest Bern: London, 1960.
(14) Zhang, L.; Manthiram, A. *Nanostruct. Mater.* **1996**, *7*, 437−451.
(15) Sonobe, N.; Kyotani, T.; Hishiyama, Y.; Shiraishi, M.; Tomita, A. *J. Phys. Chem.* **1988**, *92*, 7029−7034.
(16) Tributh; Lagaly, G. *Fachz Lab.* **1993**, *30*, 524−529, 771−776.
(17) Ece, O. I.; Alemdar, A.; Güngör, N.; Hayashi, S. *J. Appl. Polym. Sci.* **2002**, *86*, 341−346.
(18) van Olphen, H. *An Introduction to Clay Colloid Chemistry*; Krieger: Malabar, FL, 1991.
(19) Uyeda, C.; Takeuchi, T.; Yamagishi, A.; Date, M. *J. Phys. Soc. Jpn.* **1991**, *60*, 3234−3237.
(20) Longworth, G.; Townsend, M. G.; Ross, C. A. M. *Hyperfine Interact.* **1986**, *28*, 451−454.
(21) Lee, W. Y.; Tatarchuk, B. J. *Hyperfine Interact.* **1988**, *41*, 661−664.
(22) Esmer, K.; Yeniyol, M. *Mater. Lett.* **1999**, *38*, 445−449.

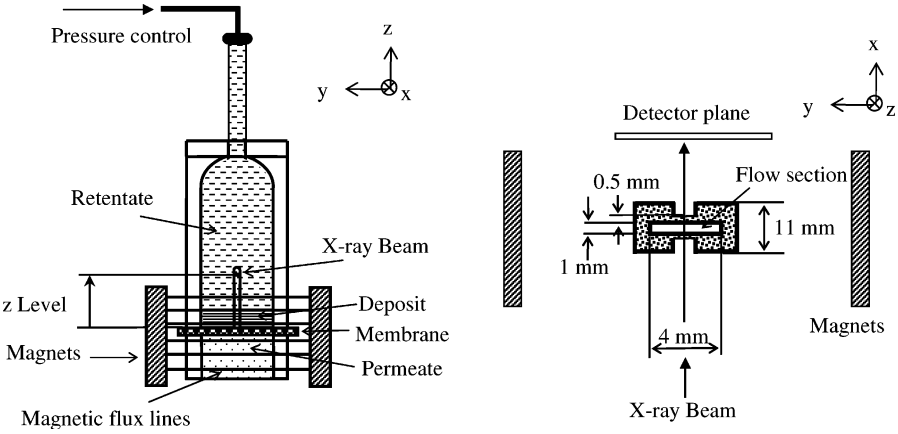

Figure 1. Schematic diagram of the frontal ultrafiltration cell developed for the in situ investigation of the deposit by small-angle X-ray scattering in a magnetic field.

20 mm). The flow section had dimensions of 4 mm × 1 mm. The flat asymmetric organic ultrafiltration membrane was made of polysulfone (Amicon, Millipore, 50 nm). Transmembrane pressure (5×10^4 Pa) was applied at the top of the column of fluid by purified compressed air. The solvent flow rate through the membrane and the deposit was measured from the time variation of the retentate fluid meniscus in the reservoir tube with an accuracy of 0.05 mL. The mean size of the particles (2 × 500 nm) is larger than the mean diameter of the membrane pores (50 nm), which prevented possible internal fouling. The cell was placed in the magnetic field, and the entire setup was translated across the X-ray beam to probe different heights of the deposit without altering the magnetic field. The magnetic field was applied perpendicular to the beam direction and the axis of the filtration cell as indicated in Figure 1. The filtration cell was placed at the geometric center of the field. The magnetic setup consisted of a stack of five magnetic elements mounted on either side of a motorized jaw. The field strength (**B**) was calibrated as a function of the gap between the opposite elements. This setup can provide a uniform field up to 1.43 T over a volume of 1 cm^3. All the measurements were performed at room temperature (22 ± 1 °C).

Small-Angle and Ultra-Small-Angle X-ray Scattering. Scattering techniques can be used to probe the different length scales involved in these charged platelike particles and their structural arrangements.[23−26] SAXS and ultra-SAXS (USAXS) measurements were carried out at the High-Brilliance Beamline (ID2) at the European Synchrotron Radiation Facility (ESRF) in Grenoble, France.[27] SAXS measurements were performed using a pinhole camera with a two-dimensional (2-d) detector, and USAXS profiles were obtained by a Bonse-Hart camera with two crossed-analyzers. The standard procedures for data acquisition and data treatment are described elsewhere.[27] All the measurements were carried out using an incident X-ray wavelength (λ) of 0.995 Å, and for SAXS two different sample-to-detector distances (2 and 10 m) were used. To obtain good position sensitivity along the vertical direction, the beam size was reduced to 0.1 mm vertically and 0.3 mm horizontally. The SAXS and USAXS measurements covered useful scattering wave vector (Q) ranges from 2×10^{-2} to 1 nm^{-1} and from 10^{-3} to 2×10^{-1} nm^{-1}, respectively. Here, the scattering vector is defined by $Q = (4\pi/\lambda) \sin(\theta/2)$, where θ is the scattering angle. The combined background due to the filtration cell and the camera was removed from each measured SAXS pattern. Furthermore, all the measured intensities were normalized to an absolute scale.[27] SAXS patterns were recorded at different positions above the membrane during the filtration process in the presence and absence of the magnetic field. The patterns provided the structural evolution of the colloidal dispersion under different conditions. To determine the magnitude of the anisotropy along parallel and perpendicular directions to the membrane, the scattering along the vertical (I_v) and horizontal (I_h) axes was calculated by integrating the scattered intensity along a sector of 30° around the vertical (z) and horizontal (y) axes, respectively. For comparison, the anisotropic level was represented by the mean value of I_v and I_h over a fixed Q range ($Q = 0.04-0.1$ nm^{-1}). The anisotropy parameter is then defined by the ratio of these two mean values (I_v/I_h). For the static experiments, the orientation of the clay particles was checked under different magnetic field strengths (0−1.43 T) in thin-walled capillaries (diameter ∼ 1.5 mm). In the ultrafiltration experiments, the empty cell was placed in the magnetic field and the background scattering was measured. The cell was then filled with the sample, and a pressure difference of 5×10^4 Pa was applied to the retentate. SAXS patterns were taken at different z positions from 0.2 to 4 mm above the membrane at different time intervals for about 3 h.

Results and Discussions

SAXS Measurements of Clay Dispersions under Static Conditions. Background-subtracted 2-d SAXS patterns from purified montmorillonite and Fe-montmorillonite under magnetic fields of different strengths are shown in Figure 2a. The effect of the magnetic field is very pronounced for the Fe-montmorillonite samples, while purified montmorillonite remained unperturbed for the highest field used. The alignment effects for the Fe-montmorillonite dispersion appeared around 0.25 T for the conditions studied here ($C = 1 \times 10^{-3}$ g mL^{-1}). The effect is reversible, and the isotropic patterns can be retrieved when the field is turned off. At this low concentration, the interparticle interactions are not affected by the applied magnetic field. To quantify the orientation effect, integrated azimuthal sector intensities were used to calculate the anisotropy parameter shown in Figure 2b. The alignment effect increases with the magnitude of the applied magnetic field. To correlate the measured SAXS intensity to the concentration of the particles within the deposit, static measurements were performed for several different clay concentrations. The measured intensities over the range 2×10^{-2} $nm^{-1} < Q < 1$ nm^{-1} were found to scale linearly with the concentration of the particles. Therefore, the mean of the radial integrated scattering intensity over the Q range extending from 0.10 to 0.20 nm^{-1} also increases linearly with the concentration of the particles as depicted in Figure 2c. The concentration of the particles within the deposits can be estimated from this integrated intensity.

SAXS and USAXS data for the dispersions of purified montmorillonite and Fe-montmorillonite under static conditions are shown in Figure 3. The intensities show

(23) Carrado, K. A.; Xu, L.; Gregory, D. M.; Song, K.; Seifert, S.; Botto, R. E. *Chem. Mater.* **2000**, *12*, 3052−3059.
(24) Xu, Y.; Hiew, P. L.; Klippenstein, M. A.; Koga, Y. *Clays Clay Miner.* **1996**, *44*, 197−213.
(25) Gazeau, F.; Dubois, E.; Bacri, J. C.; Boue, F.; Cebers, A.; Perznski, R. *Phys. Rev. E* **2002**, *65*, 031403-15.
(26) Ramsay, J. D. F.; Swanton, S. W.; Bunce, J. *J. Chem. Soc., Faraday Trans.* **1990**, *86*, 3919−3926.
(27) Narayanan, T.; Diat, O.; Boesecke, P. *Nucl. Instrum. Methods Phys. Res., Sect. A* **2001**, *467*, 1005−1009.

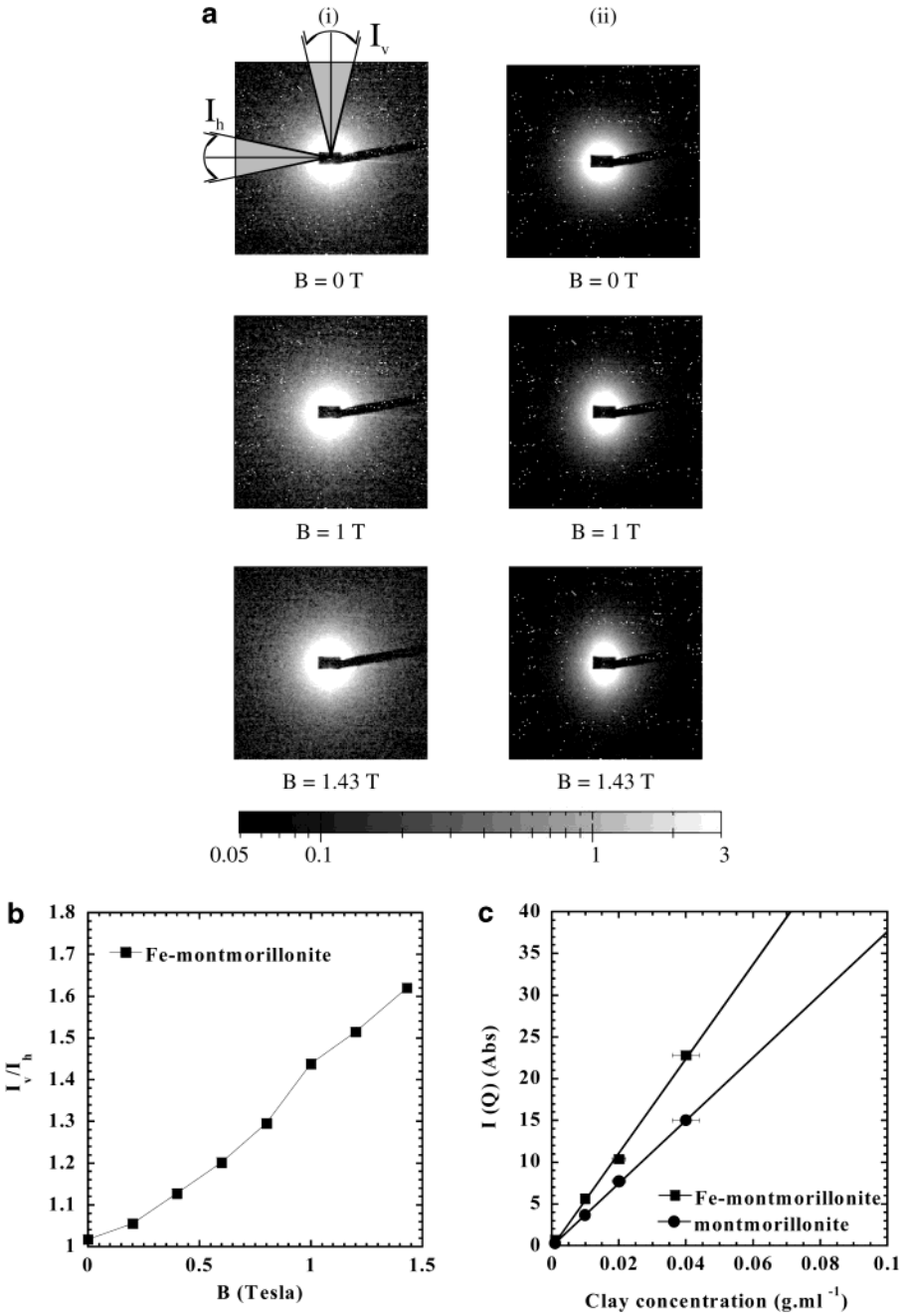

Figure 2. (a) SAXS patterns of (i) purified montmorillonite and (ii) Fe-montmorillonite dispersions in capillaries under different magnetic field strengths. $C = 10^{-3}$ g mL^{-1}, pH = 6.5. (b) Anisotropy parameter (I_v/I_h) deduced from the variation of scattering intensities I_v and I_h in absolute units from Fe-montmorillonite dispersions ($C = 10^{-3}$ g mL^{-1}, pH = 6.5) under static conditions in magnetic fields of different strengths. (c) Variation of the azimuthally averaged scattered intensity over the Q range from 0.10 to 0.20 nm^{-1} in absolute units (Abs) as a function of clay concentration for purified montmorillonite and Fe-montmorillonite under static conditions.

power law behavior over the entire Q range of measurement. For purified montmorillonite and Fe-montmorillonite, the intensity at large Q vectors (4×10^{-2} nm$^{-1} \leq Q \leq 1$ nm^{-1}) decays with exponents 2.3 and 3, respectively. For dilute randomly oriented platelike particles, the scattering intensity is expected to decay by a Q^{-2} law. The larger value of the power law exponent can be attributed to nonhomogeneous electron distribution at the interface of particles with the solvent. This effect has been demonstrated in dilute montmorillonite dispersions by Shang and Rice.[28] Furthermore, in the case of the treated Fe-montmorillonite, it may be assumed that this effect is more pronounced by the Fe^{2+} ion exchange in the crystalline structure of the particles, giving a higher discrepancy from the expected Q^{-2} power law decay.

To estimate the size of the particles, the scattering form factor $P(Q)$ was calculated for a disk of uniform density with radius R_p and height $2H_p$.[28,29] When the particles have random orientations, the single-particle scattering function may be calculated as an average over all orientations:

$$P(Q) = \int_0^{\pi/2} \frac{\sin^2(QH_p \cos \alpha_p)\, 4J_1^2(QR_p \sin \alpha_p)}{(QH_p \cos \alpha_p)^2 (QR_p \sin \alpha_p)^2} \sin(\alpha_p)\, d\alpha_p \quad (1)$$

where α_p is the angle between the axis of the disk and the

(28) Shang, C.; Rice, J. A. *Phys. Rev. E* **2002**, *64*, 021401-6.

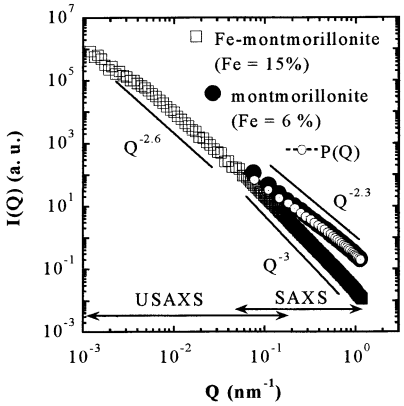

Figure 3. Small-angle and ultra-small-angle X-ray scattering from purified montmorillonite and Fe-montmorillonite dispersions in static conditions, $C = 10^{-3}$ g mL^{-1}, pH = 6.5, $\mathbf{B} = 0$ T. For comparison, the calculated form factor $P(Q)$ (eq 1) is also shown.

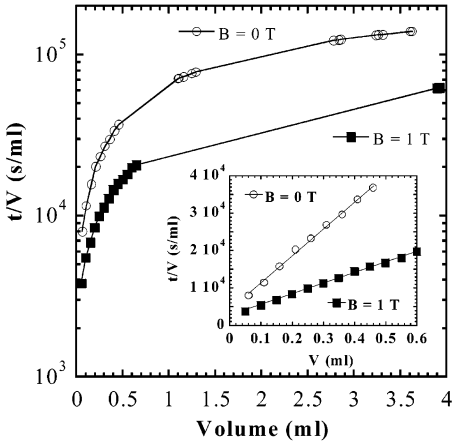

Figure 4. Filtration characteristics of Fe-montmorillonite dispersions subjected to filtration at a differential pressure of 5×10^4 Pa for 67 h as a function of magnetic field. $C = 10^{-3}$ g mL^{-1}, pH = 6.5.

scattering vector and J_1 is the first-order Bessel function. The calculated function $P(Q)$ reproduces the high Q part of the measured scattering curves with $R_p = 500$ nm and $2H_p = 2$ nm as shown in Figure 3. These values are consistent with the size of particles obtained from particle size measurements. The deviation from the calculated curve in the small Q range can be attributed to interparticle interactions.

For the Fe-montmorillonite dispersions, the intensity decays as $Q^{-2.6}$ for the Q range below 3×10^{-2} nm^{-1} as depicted in Figure 3. At this Q range, interparticle interference can be significant. In addition, the negative electron contrast at the clay−water interface[28] can also contribute to the observed deviation from single-particle behavior.

In Situ Filtration of Fe-Montmorillonite. In the filtration experiments, the purified montmorillonite and the Fe-montmorillonite dispersions were filtered at a differential pressure of 5×10^4 Pa either with or without the magnetic field for a period up to 67 h. The variation in t/V versus permeate volume is shown in Figure 4. Results show that the filtration process was intensified in a magnetic field, in comparison to the usual filtration without a magnetic field. The inset shows the specific resistance of the deposit, which is proportional to the slope

(29) Guiner, A.; Fournet, G. *Small Angle Scattering of X-Rays*; Wiley: New York, 1955.

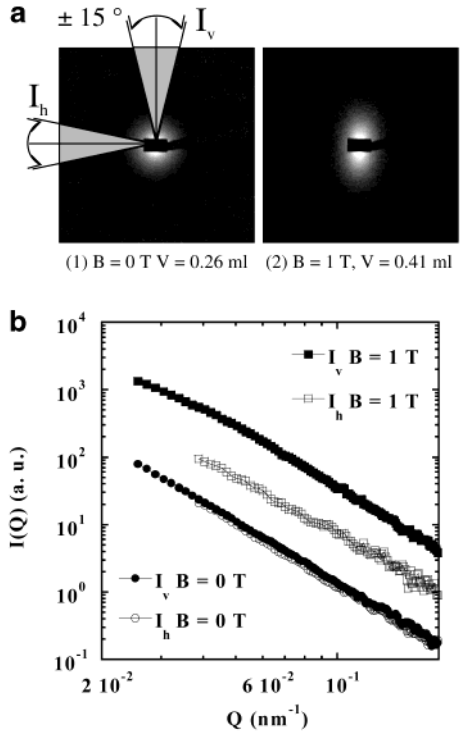

Figure 5. (a) Influence of the magnetic field on the structure of deposits formed by frontal filtration of Fe-montmorillonite ($C = 10^{-3}$ g mL^{-1}, pH = 6.5) under $P = 5 \times 104$ Pa at $z = 0.2$ mm after a filtration time $t = 5760$ s. (b) The corresponding variation of the scattering intensity I_v and I_h in absolute units.

of the curve $t/v(v)$.[1−5] For the case with a magnetic field, the slope is 2.5 times less than in the case without a magnetic field, which emphasizes the fact that the structure formed in a magnetic field has a higher porosity. The specific resistance of the cake depends largely on the particle−particle interactions and organizations. Many experimental investigations show that electrostatic interactions in particular play an important role in determining specific resistance in addition to the hydrodynamic forces due to the pressure of filtration.[1−4] In our case, the magnetic forces also act in controlling the organization of the particles. The results in Figure 4 show clearly that the magnetic field has a strong influence on the reduction of specific resistance. This effect of the magnetic field can be significant in the treatment of colloidal particles in filtration processes and in general material processing.

Influence of the Magnetic Field on Structuring of Deposits. Two types of experiments were performed for Fe-montmorillonite dispersion ($C = 1 \times 10^{-3}$ g mL^{-1}) in the same conditions of filtration: the first was in the absence of the magnetic field and the second was with a magnetic field of 1 T. Figure 5 presents the 2-d SAXS patterns 0.2 mm above the filter after 5760 s of filtration. Figure 5 shows that in the absence of a magnetic field the particles are randomly dispersed, the scattering pattern is isotropic, and the integrated scattering intensities I_h and I_v are equal for the entire Q range observed. On the other hand, during filtration under a magnetic field of 1 T, the scattering pattern is anisotropic and oriented along the vertical direction. The integrated scattering intensities I_h and I_v are higher than in the case without the field. This increase in the scattering intensity can be attributed to an enhancement of particle concentrations in the deposit. Furthermore, in the case with the field, the integrated scattering intensity I_v is 6 times higher than I_h. This increase in scattering intensity along the vertical direction can be attributed to an increase in particle

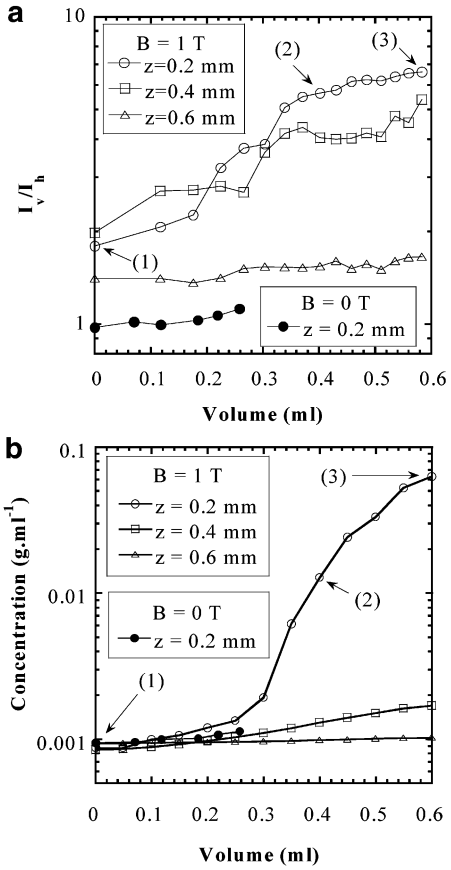

Figure 6. Characterization of deposits formed by frontal filtration of Fe-montmorillonite with and without a magnetic field. $C = 10^{-3}$ g mL^{-1}, pH = 6.5, $P = 5 \times 10^4$ Pa. Variation of (a) the anisotropy parameter (I_v/I_h) and (b) the concentration of clay in the deposit versus volume of filtered permeate, at increasing distance from the membrane.

orientation along the horizontal. This corresponds to the platelike particles predominantly oriented with their faces parallel to the membrane. The observed anisotropic pattern is typical of particles oriented uniaxially with their longer dimension along the magnetic field direction.

Figure 6 presents the anisotropy parameter and the particle concentration in the deposits versus the variation in permeate volume during the entire filtration time at a distance $z = 0.2$ mm from the membrane for the two different experiments, $\mathbf{B} = 0$ T and $\mathbf{B} = 1$ T. The anistropy parameter (I_v/I_h) was deduced from the mean of the integrated scattering intensity I_v or I_h over a Q range extending from 0.04 to 0.1 nm^{-1}. The clay concentration of the deposits was deduced from the calibration curve (Figure 2c) and from the mean azimuthally averaged intensity of the 2-d patterns over a Q range from 0.10 to 0.20 nm^{-1}. In the absence of the magnetic field, the anisotropy parameter is equal to 1 at the beginning of filtration and remains at the same level throughout the filtration process. The particle concentration in the deposit remains about 10^{-3} g mL^{-1} up to 0.26 mL of permeate volume. In experiment 2 under a 1 T magnetic field, at $z = 0.2$ mm, the anisotropy parameter is equal to 1.7 at the beginning of filtration, which emphasizes the fact that the magnetic field has oriented the particles of the initial filtering dispersion. This anisotropy parameter increases with the permeate volume, reaches a value of 3.5 for a volume of 0.26 mL, and continues to increase sharply to a value of 6.7 at 6 mL of filtered permeate volume. The particle concentration rises to 1.5 times that of the initial filtering dispersion at 0.26 mL of filtered permeate and

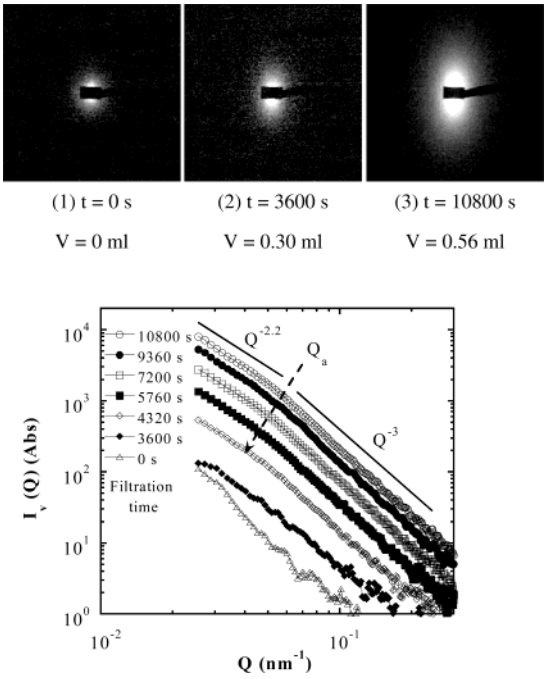

Figure 7. Time variation of SAXS patterns in frontal filtration of Fe-montmorillonite under a magnetic field, at $z = 0.2$ mm. $C = 10^{-3}$ g mL^{-1}, pH = 6.5, $P = 5 \times 10^4$ Pa, $\mathbf{B} = 1$ T. The corresponding sector-averaged intensity along the vertical axis (I_v).

reaches 65.8 times the initial concentration at 6 mL of filtered permeate. These results show that for the same filtered permeate volume of 0.26 mL, filtration in a magnetic field creates a deposit that is 3.5 times more oriented and 1.5 times more concentrated than filtration in the absence of a magnetic field. Furthermore, the deposit formed in a magnetic field has a greater permeability and the time needed to reach the same volume of filtered permeate is reduced to 2460 s from 5760 s when $\mathbf{B} = 0$ T.

For the same filtration time (5760 s) [Figures 5 and 6], the deposit formed in a magnetic field has an anisotropy parameter that is larger by a factor of 6, the particle concentration increased by a factor of 11, and the specific resistance was reduced by a factor of 2.5 [Figure 4] as compared to a deposit formed in the absence of a magnetic field. This suggests that a greater orientation of the particles in the deposit, even at a higher particle concentration, enhances the filtration performance. One explanation for this surprising effect could be that greater organization of the particles in the structure of the deposit creates preferential channels for water to flow through, thus increasing the permeability of the deposit. In the case without a magnetic field, where the particles are randomly dispersed in the deposit, one may expect to find more tortuous ways for water to drain through, thus reducing the permeability of the deposit.

In Situ SAXS Measurements of Structuring of Deposits in a Magnetic Field. Figure 7 shows the SAXS patterns and variation in integrated scattering intensity I_v during the ultrafiltration of an Fe-montmorillonite dispersion in a magnetic field of 1 T, at a short distance from the membrane, $z = 0.2$ mm.

At the beginning of filtration, the scattering pattern exhibits slight anisotropy, which further increases during filtration [Figure 7, panels 1, 2, and 3)]. The absolute level of scattering intensity I_v is enhanced during the filtration, which corresponds to an increase in particle concentration. A characteristic value of the wave vector (Q_a) separates

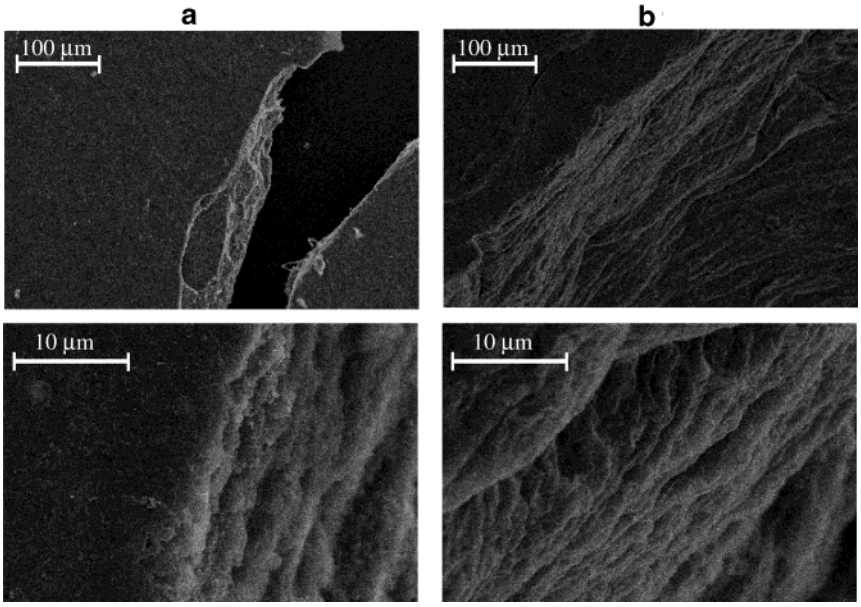

Figure 8. Scanning electron micrographs of the deposits formed in frontal filtration of an Fe-montmorillonite dispersion under 5×10^4 Pa, $\mathbf{B} = 1$ T: (a) for a filtration time of 3 h; (b) for a filtration time of 67 h.

the $Q^{-2.2}$ power law decay from Q^{-3} power law decay at higher Q ranges, and Q_a shifted to higher Q values with time. The Q^{-3} power law decay corresponds to the same behavior observed in a dispersion at rest in a capillary [Figure 3]. This Q^{-3} behavior extends over a range of Q values, corresponding to the intraparticle dimensions. Above Q_a, the decrease from the Q^{-3} to $Q^{-2.2}$ power law decay can be attributed to the contribution of interparticle interactions. The decrease of Q_a can be attributed to the decrease in the average interparticle separation. This observation is in good agreement with the fact that the deposits become more concentrated with filtration time.

Throughout the filtration process, it was possible to monitor the structural organization of the cake at different distances from the membrane. In Figure 6(a and b), the anisotropy parameter (I_v/I_h) and particle concentration in the deposit are depicted as a function of volume of the filtered permeate. For a distance above 0.6 mm from the membrane, the anisotropy parameter (equal to 1.4) and particle concentration (1×10^{-3} g mL^{-1}) remained nearly at the same level from the beginning to the end of filtration. This emphasizes the fact that the deposit formed in this experiment developed at distances below $z = 0.6$ mm. For distances $z = 0.2$ and 0.4 mm, the deposits show an increasing anisotropy parameter and particle concentration during the filtration process. At 0.6 mL volume of filtered permeate, the value of the anisotropy parameter was increased roughly by a factor of 3 at $z = 0.4$ mm and by a factor of 4 at $z = 0.2$ mm as compared to their initial values at 0 mL volume of the filtered permeate. Simultaneously, during the filtration process, there was a slight increase in particle concentration at $z = 0.4$ mm, which reached 1.7×10^{-3} g mL^{-1} at 0.6 mL, and a large increase at $z = 0.2$ mm, which reached 63×10^{-3} g mL^{-1} at 0.6 mL. These results suggest that the structural organization within the cake involves the platelike particles with their faces parallel to the membrane. If the platelets turn around along their diameter as they flow through the retentate due to hydrodynamic forces, excluded volume effects, or electrostatic interactions, then the resulting arrangement would be less anisotropic in the vicinity of the membrane. But the results show that the level of anisotropy in the deposit is similar at $z = 0.2$ and $z = 0.4$ mm throughout the course of filtration. These observations emphasize the fact that the strength of the magnetic field is the dominant factor in orienting the particles, as compared to hydrodynamic or electrostatic forces in the dispersion.[30] The uniaxial orientation is presumably arising from the combined action of the magnetic field and the excluded volume effect. Consequently, the particles pile up on one another to form a uniaxial organization which becomes progressively concentrated near the membrane.

Figure 4 shows that the specific resistance of the deposit changes linearly during the filtration, which confirms the continuous manner in which the particles form the structure of the deposit. This experiment shows that for the conditions applied here, the deposit is 37 times more concentrated in the layer at $z = 0.2$ mm than in the layer at $z = 0.4$ mm, which gives an order of magnitude ($\approx$0.2 mm) for the denser layer near the membrane that predominantly controls the filtration flow rate.

SEM Measurements of the Filtration Cake. The structure of the deposit at larger length scales can be observed by scanning electron microscopy. The deposits obtained from the filtration experiment described in the previous section were allowed to dry at room temperature, and these dry deposits were examined under an electron microscope. Figure 8 displays the scanning electron micrograph of the Fe-montmorillonite deposits obtained after 10 800 s of filtration (Figure 8a) and that obtained after 67 h of filtration (Figure 8b). The observations were made in the direction that provides a view through the thickness of the deposit parallel to the X-ray beam. The deposit formed in the magnetic field exhibits a regular horizontal ordering of the platelets. These observations confirmed the structural organization deduced from the SAXS patterns: the formation of a lamellar arrangement of platelike particles with their faces oriented parallel to the membrane.

Conclusions

The Fe-montmorillonite clay particles obtained by the cation exchange process exhibit significant orientation effects under an external magnetic field. In the absence of a magnetic field, the dispersion is composed of randomly

(30) Benna, M.; Kbir-Ariguib, N.; Clinard, C.; Bergaya, F. *Appl. Clay Sci.* **2001**, *19*, 103−120.

oriented clay particles. The measured SAXS patterns became anisotropic above 0.4 T under the conditions used in this study. On the other hand, natural montmorillonite particles remain isotropic up to the maximum value of the magnetic field applied. By measuring the SAXS intensity on an absolute scale, it is possible to correlate the intensity to the concentration of the particles within the deposits. A combination of SAXS and USAXS provided the overall structural organization within the dispersion.

In the absence of a magnetic field, the changes in SAXS intensity and its azimuthal distribution as a function of time indicated that the deposits are composed of randomly oriented particles. On the other hand, during filtration in a magnetic field, Fe-montmorillonite particles organize uniaxially with their faces oriented parallel to the membrane. The deduced concentration profile and anisotropy parameter as a function of permeate volume showed that this structure is progressively concentrated with the proximity of the membrane with a dense layer in the close vicinity of the membrane. Simultaneously, the filtration curves show that application of the magnetic field reduces the specific resistance of the deposit by a factor of 2.5, thereby enhancing the filtration flow rate. This suggests that well-oriented structures, even at the highest particle concentrations, lead to better filtration performance.

Further experiments using more monodisperse anisotropic colloidal particles will aid in obtaining a better understanding of the mechanism of self-organization of particles during the filtration process. The strong effect of an applied magnetic field on the filtration process offers new opportunities for the treatment of colloidal particles in membrane processes and the development of nanomaterial fabrication.

Acknowledgment. The authors express their deepest thanks to the French Ministry of Research and to the "Département des Sciences pour l'Ingénieur" of the CNRS, who supported this work. The European Synchrotron Radiation Facility is acknowledged for SC866 beam time allocation. We thank P. Panine and J. Gorini for technical assistance and I. Snigireva for the SEM images.

LA030020P